



HAL
open science

Theoretic-Information Entropies Analysis of Nanostructures: Ab Initio Study of PAMAM Precursors and Dendrimers G0 to G3

Rodolfo O Esquivel, Nelson Flores-Gallegos, Edmundo Carrera, Catalina Soriano-Correa, Juan Carlos Angulo, Jesus S Dehesa, Juan Antolin

► **To cite this version:**

Rodolfo O Esquivel, Nelson Flores-Gallegos, Edmundo Carrera, Catalina Soriano-Correa, Juan Carlos Angulo, et al.. Theoretic-Information Entropies Analysis of Nanostructures: Ab Initio Study of PAMAM Precursors and Dendrimers G0 to G3. *Molecular Simulation*, 2009, 35 (06), pp.498-511. 10.1080/08927020902833087 . hal-00515081

HAL Id: hal-00515081

<https://hal.science/hal-00515081>

Submitted on 4 Sep 2010

HAL is a multi-disciplinary open access archive for the deposit and dissemination of scientific research documents, whether they are published or not. The documents may come from teaching and research institutions in France or abroad, or from public or private research centers.

L'archive ouverte pluridisciplinaire **HAL**, est destinée au dépôt et à la diffusion de documents scientifiques de niveau recherche, publiés ou non, émanant des établissements d'enseignement et de recherche français ou étrangers, des laboratoires publics ou privés.

**Theoretic-Information Entropies Analysis of
Nanostructures:
Ab Initio Study of PAMAM Precursors and Dendrimers G0 to
G3**

Journal:	<i>Molecular Simulation/Journal of Experimental Nanoscience</i>
Manuscript ID:	GMOS-2008-0226.R1
Journal:	Molecular Simulation
Date Submitted by the Author:	13-Feb-2009
Complete List of Authors:	Esquivel, Rodolfo; Universidad de Granada, Physics; Universidad Autonoma Metropolitana, Chemistry Flores-Gallegos, Nelson; UAM, Chemistry Carrera, Edmundo; UAM, Chemistry Soriano-Correa, Catalina; UNAM, FES-Zaragoza Angulo, Juan; Universidad de Granada, Physics Dehesa, Jesus; Universidad de Granada, Physics Antolin, Juan; Universidad de Zaragoza, Departamento de Física Aplicada
Keywords:	Nanostructures, Dendrimers, PAMAM, Information Theory, Ab initio Calculations

SCHOLARONE™
Manuscripts

1
2
3
4
5
6
7
8
9
10
11
12
13
14
15
16
17
18
19
20
21
22
23
24
25
26
27
28
29
30
31
32
33
34
35
36
37
38
39
40
41
42
43
44
45
46
47
48
49
50
51
52
53
54
55
56
57
58
59
60

Theoretic-Information Entropies Analysis of Nanostructures: Ab Initio Study of PAMAM Precursors and Dendrimers G0 to G3

R. O. Esquivel^{*1,2,3}, N. Flores-Gallegos³, E.M. Carrera³,
J.S. Dehesa^{1,2}, J.C. Angulo^{1,2}, J. Antolín^{2,4} and C. Soriano-Correa⁵

¹ *Departamento de Física Atómica, Molecular y Nuclear, Universidad de Granada*
18071-Granada, Spain

² *Instituto Carlos I de Física Teórica y Computacional, Universidad de Granada, 18071-Granada, Spain*

³ *Departamento de Química, Universidad Autónoma Metropolitana-Iztapalapa*
San Rafael Atlixco No. 186, Col. Vicentina, C.P. 09340, México D.F.

⁴ *Departamento de Física Aplicada, EUITIZ, Universidad de Zaragoza, 50018-Zaragoza, Spain*

⁵ *Laboratorio de Química Computacional, FES-Zaragoza, Universidad Nacional Autónoma de México, C.P.*
09230 Iztapalapa, México, D.F., México

1
2
3
4
5
6
7
8 **Abstract.** Information Theory (IT) in conjugated and in Hilbert spaces is employed to analyze the
9 growing behavior of nanostructures. Shannon entropies in position and momentum spaces require
10 costly and time-consuming computations as the size of the molecules increases in contrast with
11 information entropies in Hilbert space, which are shown to be highly advantageous for analyzing
12 large molecules. In this work, *ab initio* electronic structure calculations at the HF, MP2 and B3LYP
13 levels of theory were performed to analyse the initial steps towards growing nanostructured
14 molecules of Polyamidoamine (PAMAM) dendrimers, starting from the monomers, dimers,
15 trimers, tetramers up to generations G0 (with 84 atoms), G1 (228 atoms), G2 (516 atoms), and G3
16 (1092 atoms). This is achieved by using selected physical descriptors such as the radius of gyration,
17 the asphericity factor, the moments of inertia, the dipole moments, the total energies and chemical
18 reactivity indices such as the hardness, softness and the electrophilicity index at the HF/3-21G*
19 level of theory. For the chemical indices, higher level calculations at the B3LYP/6-311++G** and
20 MP2/6-311+G* levels were also performed in order to account for the effects of electron
21 correlation. Information-theoretic measures of the Shannon type in conjugated space are employed
22 to characterize the G0-PAMAM precursors and G0. Hilbert space entropies of the Shannon and
23 Kullback type are employed to provide theoretic-information evidence of the validity of the dense-
24 core model of PAMAM precursors and dendrimers G0 through G3.
25
26
27
28
29
30
31
32
33
34
35
36
37
38
39
40
41
42
43
44
45
46
47
48
49
50
51
52
53
54
55
56
57
58
59
60

Keywords: Nanostructure, Dendrimers, PAMAM, Information Theory, Ab Initio Calculations

INTRODUCTION

Since their introduction in 1985 by Tomalia et al. [1], dendrimers have attracted much attention because of their fascinating structure and unique properties [2]. Dendrimers are globular, size monodisperse macromolecules in which all bonds emerge radially from a central focal point or core with a regular branching pattern and with units that repeat and contribute to a branch point. They are defined by three components: a central core, an internal dendritic structure (the branches), and an external surface with functional surface groups. Not all regularly branched molecules are dendrimers because properties of the dendritic state [2b], such as core encapsulation [3]. These macromolecules were first synthesized in the early 1980s with the development of a cascade type of synthetic strategies to give distinct generations (G0, G1, G2, ...) of molecules with narrow molecular weight distribution, uniform size and shape, and multiple (multivalent) surface groups.[4]. Several applications for dendrimers have been proposed in the literature [5], with potential applications in biology as mimetic systems of enzymes or redox proteins [6], in medicine for drug delivery, gene therapy, and biochemical sensors [7], in optoelectronics for transduction of signals or light-harvesting devices [8] and in nanoscience as building units in self-assembled systems or functionalized with groups for molecular recognition and signaling [5a,5b,9].

Poly(amido)amine or PAMAM dendrimers are among the most studied families of dendrimers. These organic dendrimers contain tertiary amines as branching points, i.e., the respective branching multiplicity is 2. The core multiplicity varies; the original PAMAM dendrimers were synthesized from an amine core and thus had a 3-fold multiplicity [1,6a] whereas recently, ethylenediamine-core PAMAMs became more common and these possess a 4-fold multiplicity where the typical end-groups are primary amines [10].

1
2
3
4
5
6
7
8 A number of review articles on dendrimers have been reported [5,8a,11]. Most of the reported
9
10 work was motivated by a dendrimer-model of a hollow core and hence by a dense shell. The basic
11
12 assumption behind this was that the density of the segments increases from the center to the
13
14 periphery, supporting the idea of using dendrimers as dendritic boxes or carriers. This dense-shell
15
16 model became popular since the work of de Gennes and Hervet [12] in which they presented the
17
18 first theoretical treatment of dendrimers by using a modified version of self-consistent field (SCF)
19
20 method developed by Edwards [13] where they obtained a density profile with a global minimum at
21
22 the center and a monotonic density increasing towards the periphery of the dendrimer. Much of the
23
24 work on synthesis of dendrimers and applications indicates that most studies are still based on this
25
26 assumption. On the other hand, Lescanec and Muthukumar performed the first simulations of
27
28 dendrimers [14]. They used a kinetic growth algorithm of self-avoiding walks to build off-lattice
29
30 dendrimers and they found, in contrast with Ref. [12], density profiles that decreased monotonically
31
32 towards the edge of the molecule. They were the first to show that a dendritic structure made up
33
34 from flexible bonds should exhibit its maximum density at the center of the molecule (dense-core
35
36 model). This pioneering work has been the starting point of a considerable number of theoretical
37
38 studies which support the early result of Lescanec and Muthukumar, thus firmly establishing the
39
40 validity of the dense-core model.
41
42
43
44
45
46
47
48

49 Several theoretical approaches have been applied to the problem of the conformation of isolated
50
51 dendrimers, the Self-Consistent Field method (SCF) [12,15], the Gaussian variational approximation
52
53 (GVA) [16] and the Gaussian self-consistent theory (GSC) [17]. Except for the work of de Gennes
54
55 and Hervet [12], all of them support the dense-core model. Furthermore, a great deal of progress in
56
57 the understanding of the conformations of dendrimers has been achieved through computer
58
59
60

1
2
3
4
5
6
7
8
9
10
11
12
13
14
15
16
17
18
19
20
21
22
23
24
25
26
27
28
29
30
31
32
33
34
35
36
37
38
39
40
41
42
43
44
45
46
47
48
49
50
51
52
53
54
55
56
57
58
59
60

simulations at various levels of description, from the microscopic (atomistic) to the oversimplified ones with different methodologies: Monte-Carlo (MC), molecular dynamics (MD), and Brownian dynamics (BD) [18]. Recently, Maiti et al [19], performed a systematic series of fully atomistic MC-MD simulations on PAMAM-ethylenediamine (PAMAM-EDA) cored dendrimers from G0 through G11, to characterize the structure and properties of these molecules. They reported the cartesian coordinates for a snapshot of the trajectory for each dendrimer from generation 3 to generation 11. On the electronic structure (ES) side, only a few Hartree-Fock (HF) and density functional theory (DFT) studies have addressed to study some structural, thermodynamic, electronic and vibrational aspects of low order generation dendrimers (G0 and G1) [20]. To the best of our knowledge, there are no *ab initio* studies of the ES type which address the problem of understanding the structural properties of PAMAM dendrimers of higher generations and the issue is not a simple one since these molecules possess an enormous number of energetically permissible conformations and a large number of atoms (EDA-PAMAM dendrimers grow from 84 atoms for G0 up to 294852 atoms for G11) which are beyond the present capabilities for the ES packages and present computers to attempt high level *ab initio* calculations, notwithstanding it remains a major goal of quantum chemistry to design strategies and methodologies which could be applied to dendrimers of higher generations. These molecules have now become an important issue in the fields of polymer theory, the physics of soft matter and supramolecular chemistry.

A most challenging problem for Chemistry and Physics resides in characterizing and measuring the interactions between the different parts of a quantum system which are thought as those essential pieces of the whole system which may explain the chemical reactivity and how to construct the formalism of more complex systems through the interplay of its constituting parts. In Quantum Chemistry, the concept of Atoms in Molecules (AIM) has been the focus of great deal of attention

[21] since it provides a natural framework to study chemical reactivity of complex molecules by means of the interactions between atoms or functional groups and between different molecules when small density changes are produced. The real space partitioning of a molecule into subsystems is still a challenging problem in theoretical chemistry [21,22], not only because of the arbitrary chemical frontiers that separate subsystems but also because of the high computational cost that is involved in the calculations. Atomic orbital-based population analyses are very popular in chemistry and though they allow for the partition of the molecular wave function into atomic contributions, they are not rotationally invariant and may produce negative populations [23]. However, there exist alternative schemes which avoid these drawbacks, for instance the natural atomic orbital scheme of Weinhold [24] or the one of Davidson-Löwdin [25]. For this purpose, Löwdin symmetric orthogonalization on the atomic orbitals of the same atom has been considered most useful [26]. In defining these schemes one can preserve to a maximum extent the information content of ground state atoms to obey physical principles such as the N- and v-representability. Further, information-theoretic principles can be employed to define suitable natural probabilities for analyzing interactions between molecular units or fragments in a molecule, which in turn allow for more involved chemical studies such as reactivity, conformational analysis, similarity, reactions, dissociation processes, etc. [27]. To the best of our knowledge and notwithstanding that there has been a great interest in the last years in applying Information Theory (IT) measures to the electronic structure of atoms and molecules in a wide variety of fields [28], no IT studies have been performed on nanostructures of the dendrimer type.

Through the present investigation we will show that despite the limitations of quantum chemistry methods, it is possible to apply chemical concepts to elucidate some of the structural

1
2
3
4
5
6 features of dendrimers. One of the goals is to support the validity of the core-dense model for
7
8 dendrimers from a theoretic information point of view. Besides, we will employ some selected
9
10 polymer science properties of dendrimers to reveal the growing behavior of PAMAM precursors
11
12 and the G0 dendrimer at the HF level of theory along with several chemical reactivity parameters
13
14 within the context of conceptual DFT. Higher level calculations at the DFT-B3LYP and MP2 levels
15
16 of theory will be attempted to take into account the effects of electron correlation on the chemical
17
18 indices. Finally, we will show that information entropies in Hilbert space are able to reveal the
19
20 growing behavior of PAMAM-EDA nanostructures up to G3 with significant computational
21
22 advantages as compared to the calculation of standard Shannon entropies in position and
23
24 momentum spaces.
25
26
27
28
29
30
31
32

33 THEORETICAL DETAILS

34
35
36
37 Throughout the study we will employ several physical descriptors commonly used in polymer
38
39 science and in theoretical chemistry which will be defined in this section. The principal moments of
40
41 inertia I_x , I_y and I_z are calculated through the eigenvalues of the shape tensor G describing the
42
43 mass distribution:
44
45
46
47
48

$$49 G_{pq} = (1/M) \left[\sum_i^N m_i (r_{pi} - R_p)(r_{qi} - R_q) \right] \quad (1)$$

50
51
52
53

54
55 where $p, q = x, y, z$, and r_{pi} is the position of the i th atom relative to the R_p components of the center
56
57 of mass of the molecule, M is the mass of the molecule and m_i is the mass of the atom. The sum of
58
59
60

three eigenvalues (I_x , I_y and I_z) is an invariant of the shape tensor \mathbf{G} , giving $\langle R_g^2 \rangle$, which is the mean-square radius of gyration that provides a quantitative characterization of the dendrimer size. The ratio of these three principal moments is a measure of *eccentricity* (minor-major axes ratio) of the shape ellipsoid of the dendrimers and hence the shape of the dendrimer can be assessed from the values of the ratio of the three principal moments of inertia of the molecules I_x/I_y and I_x/I_z . Rudnick and Gaspari [29] introduced a better definition of *asphericity* frequently used in the literature as

$$\delta = 1 - 3 \frac{\langle I_2 \rangle}{\langle I_1^2 \rangle} \quad (2)$$

where I_i are the respective invariants of the gyration tensor and are given by

$$I_1 = I_x + I_y + I_z \quad (3)$$

and

$$I_2 = I_x I_y + I_x I_z + I_y I_z \quad (4)$$

We have also evaluated some reactivity parameters that may be useful to analyze the chemical properties of the precursors. Parr and Pearson proposed a quantitative definition of hardness (η) within conceptual DFT [30]:

$$\eta = \frac{1}{2S} = \frac{1}{2} \left(\frac{\partial \mu}{\partial N} \right)_{v(r)} \quad \text{where} \quad \mu = \left(\frac{\partial E}{\partial N} \right)_{v(r)} \quad (5)$$

is the electronic chemical potential of an N electron system in the presence of an external potential $v(r)$, E is the total energy and, in the context of density functional theory, “ S ” is called the softness. Using finite difference approximation, Eq. (9) would be

$$\eta = \frac{1}{2S} \approx (E_{N+1} - 2E_N + E_{N-1}) / 2 = (I - A) / 2 \quad (6)$$

where E_N , E_{N-1} and E_{N+1} are the energies of the neutral, cationic and anionic systems, and I and A , are the ionization potential (IP) and electron affinity (EA), respectively. Applying Koopmans’ theorem [31] Eq. (6) can be written as:

$$\eta = \frac{1}{2S} \approx \frac{\varepsilon_{LUMO} - \varepsilon_{HOMO}}{2} \quad (7)$$

where ε denotes the frontier molecular orbital energies. In general terms, hardness and softness are good descriptors of chemical reactivity, the former measures the global stability of the molecule (larger values of η means less reactive molecules), whereas the “ S ” index quantifies the polarizability of the molecule [32], thus soft molecules are more polarizable and possess predisposition to acquire additional electronic charge [33]. The chemical hardness “ η ” is a central quantity for use in the study of reactivity and stability, through the hard and soft acids and bases principle [34].

On the other hand, Parr et al. [35] have defined another descriptor in order to quantify the global electrophilic power of the molecules, namely the electrophilicity index ω , which defines a quantitative classification of the global electrophilic nature of a molecule within a relative scale. Electrophilicity index of a system in terms of its chemical potential and hardness is given by the next expression:

$$\omega = \frac{\mu^2}{2\eta} \quad (8)$$

In general terms, hardness and electrophilicity are good descriptors of chemical reactivity, the former measures the global stability of the molecule (larger values of η means less reactive molecules), whereas the ω index quantifies the global electrophilic power of the molecules (predisposition to acquire an additional electronic charge) [33]

According to the goals of the present study, the central quantities in real space are the Shannon entropies, either in position or momentum spaces [36]:

$$S_r = -\int \rho(\mathbf{r}) \ln \rho(\mathbf{r}) d^3\mathbf{r} \quad (9)$$

$$S_p = -\int \gamma(\mathbf{p}) \ln \gamma(\mathbf{p}) d^3\mathbf{p} \quad (10)$$

where $\rho(\mathbf{r})$ and $\gamma(\mathbf{p})$ are normalized to unity and denote the molecular electron density distributions in the position and momentum spaces, respectively. The Shannon entropy behaves like a measure of delocalization or lack of structure of the electronic density in the position space and

1
2
3
4
5 hence S_r is maximal when knowledge of $\rho(\mathbf{r})$ is minimal. The Shannon entropy in momentum space
6
7
8 S_p is largest for systems with electrons of higher speed and is smaller for relaxed systems where
9
10 kinetic energy is low. Entropy in momentum space S_p is closely related to S_r by the uncertainty
11
12 relation of Bialynicki-Birula and Mycielski [37] which shows that the entropy sum $S_T=S_r+S_p$, is a
13
14 balanced measure and cannot decrease arbitrarily. For one-electron atomic systems it may be
15
16 interpreted as that localization of the electron's position results in an increase of the kinetic energy
17
18 and a delocalization of the momentum density.
19
20

21
22 From a different perspective, we have recently shown [27] that there is an information-theoretic
23
24 justification for performing Lowdin symmetric transformations [38] on the atomic Hilbert space, to
25
26 produce orthonormal atomic orbitals of maximal occupancy for the given wavefunction, which are
27
28 derived in turn from atomic angular symmetry subblocks of the density matrix, localized on a
29
30 particular atom and transforming to the angular symmetry of the atoms. The advantages of these
31
32 kind of atoms-in-molecules (AIM) approaches [39,40] are that the resulting natural atomic orbitals
33
34 are N-representable, positively bounded, and rotationally invariant [25,41]. In consequence, we
35
36 have also shown [42] that the corresponding "natural atomic probabilities" (NAP) are useful to
37
38 define von Neumann information entropies in Hilbert space which are able to measure
39
40 entanglement in the context of Quantum Information Theory [43].
41
42
43

44
45 The uncertainty of a probability distribution $p_i(A)$ is measured through the Shannon entropy in
46
47 Hilbert space [44]:
48
49
50

$$51 \quad H(A) = -\sum_i p_i(A) \ln p_i(A) \quad (11)$$

52
53
54
55
56
57
58
59
60

The relative entropy between two probability distributions $p_i(A)$ and $p_i(B)$ is defined through the Kullback-Liebler entropy [45] as

$$H(A\|B) = \sum_i p_i(A) \ln \frac{p_i(A)}{p_i(B)} \quad (12)$$

where the $p_i(A)$ (and $p_i(B)$) in Eqs. (11) and (12) can be determined by use of natural atomic probabilities [27,42]. It is worth noting that while Eq. (12) represents a distance from a reference probability, it fails to be symmetric.

RESULTS AND DISCUSSION

The electronic structure calculations performed in this study were carried out with the NwChem suite of programs [46] at the HF/3-21G* and B3LYP/6-311++G** levels of theory and with the Gaussian/G03 suite of programs [47] for calculations at the MP2/6-311+G* level of theory. The systems under analysis are precursors of PAMAM-EDA G0, i.e., EDA ($C_2H_4(NH_2)_2$), the PAMAM monomer ($NH_2-CH_2-CH_2-CO-NH-CH_2-CH_2-NH_2$), the dimer (EDA+monomer), the trimer (EDA+ 2 monomers), and the tetramer (EDA+ 3 monomers) along with some of the conformers of these systems, which were optimized at the levels of theory required for each property as mentioned below. The G0 geometry for the IT study in real space along with the geometries G1 through G3 employed for the IT study in Hilbert space were obtained from Maiti [19,48] and then calculated at the HF/3-21G* level [46]. In order to determine the information entropies in Hilbert

1
2
3
4
5 space, $H(A)$ and $H(A|B)$, we employed natural atomic probabilities [27] calculated with the NBO
6
7
8 5.G software [49]. The molecular Shannon information entropies in position and momentum spaces
9
10 were obtained by employing software developed in our laboratory along with the 3D numerical
11
12 integration routines by Pérez-Jordá et al [50] and the DGRID suite of programs by Kohout [51].
13
14 Besides, several electronic structure properties were calculated in order to analyze the shape of the
15
16 polymers, the aspect ratios, the asphericity factor, and the dipole moment components, along with
17
18 several DFT chemical reactivity properties such as the frontier orbital energies (HOMO and
19
20 LUMO), hardness, softness and the electrophilicity values. Since these chemical properties might be
21
22 sensitive to the electron correlation and basis set quality we have performed calculations at the
23
24 MP2/6-311+G* and B3LYP/6-311++G** levels of theory. Optimized structures at each level were
25
26
27 determined in order to obtain reliable values for chemical reactivity parameters.
28
29
30
31
32

33
34 In Table 1 we have reported the total dipole moment values for all polymeric structures from
35
36 EDA through G0 along with the dipole moment components which are also shown in Figure 1
37
38 from which we can witness an increase of the polarization of the molecular densities in all directions
39
40 as the molecules grow, with larger effects for G0. This might be indicative of more polarizable
41
42 densities which in turn may reflect molecular densities that tend to be more delocalized.
43
44
45
46
47
48
49
50
51
52
53
54
55
56
57
58
59
60

Table 1. Values for the total dipole moment and its components [Debye] for the PAMAM-G0 precursors and G0 dendrimer calculated at the HF/3-21G* level of theory.

<i>Molecule</i>	μ_x	μ_y	μ_z	μ_{TOTAL}
EDA	0.0	0.0	0.0	0.0
M1	-0.477	0.745	0.699	3.365
M2	1.073	0.702	0.594	2.509
M3	1.073	0.702	0.594	5.826
M4	0.042	0.916	0.481	2.368
M5	-0.216	0.644	0.969	2.583
D1	-0.814	-1.678	4.490	4.479
D2	1.131	-3.314	-0.221	4.334
T1	0.164	0.893	1.389	2.267
T1T1	3.114	-0.450	-1.227	3.377
T1T2	4.729	1.060	1.075	4.964
G0	3.041	-7.293	1.488	3.241

It is known that flexible-chain dendrimers, although being chemically regular structures, do not assume regular shapes. To quantitatively evaluate the deviation from spherical symmetry, we calculated the shape of the precursors and G0 dendrimer through several physical quantities: the principal moments of inertia I_x , I_y and I_z (Eq. 1), the ratio of the three principal moments of inertia of the molecules I_z/I_y and I_z/I_x , the asphericity factor (Eq. 2) and the dendrimer size (measured through the radius of gyration which is the mean-square of the sum of the moments of inertia). The values of the three principal moments of inertia are tabulated in Table 2, along with the radius of

gyration and the asphericity factor, while Figures 2 through 4 show the moment of inertia ratios, the radius of gyration and the asphericity factor, respectively, for the different G0-precursors and the G0 dendrimer.

TABLE 2. Values for the principal moments of inertia I_x , I_y , I_z [a.u.], the radius of gyration (R_g) [a.u.], and the parameter of asphericity δ for the precursors and dendrimer G0 calculated at the HF/3-21G* level of theory.

<i>Molecule</i>	I_x	I_y	I_z	R_g	δ
EDA	486	71	495	32.4	0.159
M1	3001	1044	2823	82.8	0.075
M2	2089	3218	1571	82.9	0.045
M3	2090	3218	1571	82.9	0.045
M4	1762	1574	1813	71.8	0.002
M5	1721	3028	1965	81.9	0.032
D1	3152	5286	6231	121.1	0.035
D2	5174	2142	6782	118.7	0.084
T1	14936	18993	32820	258.4	0.059
TT1	21767	26043	42123	300.0	0.043
TT2	28212	20641	43350	303.6	0.047
G0	42929	46745	26720	341.2	0.025

From Table 2 and Figure 2 we may assess the size of the dendrimers through the radius of gyration. As expected, R_g values show a constant increasing trend in going from the monomers up

to the G0-dendrimer. The shape of the G0-precursors and G0 dendrimer can be assessed from the values of the ratio of the three principal moments of inertia of the molecules I_z/I_y and I_z/I_x in Figure 3 from which we observe that all the precursors are more eccentric than the G0 generation, which tend to be more spherical. A quantity which reflects this fact in a more precise manner is the asphericity factor, which is depicted in Figure 4, where it may be observed that dendrimer G0 tend to be more spherical as compared to the rest of the G0-precursors, except for the M4 monomer whose conformeric structure is not linear.

On the chemical side we have also evaluated some reactivity parameters that may be of utility to analyze the chemical properties of the precursors. In general terms, hardness and electrophilicity are good descriptors of chemical reactivity, the former measures the global stability of the molecule (larger values of η means less reactive molecules), whereas the ω index quantifies the global electrophilic power of the molecules (predisposition to acquire an additional electronic charge) [33]. In Table 3 we have reported values for the total energies, the frontier orbital energies HOMO and LUMO, the hardness and the electrophilicity index. These values were calculated at three different levels of theory: HF/3-21G*, B3LYP/6-311++G** and MP2/6-311+G* in order to take into account with the effects of electron correlation. It is worth mentioning that geometry optimization for each precursor was performed at every level of theory. The different values are reported in Table 3 for comparison purposes. Also, we have depicted the values for the hardness and the electrophilicity index in Figures 5 and 6, respectively, at the HF, B3LYP and MP2 levels of theory as to analyse the general trends and also the effects for electron correlation.

TABLE 3. Values for the total energies, frontier orbital energies, hardness (η) and the electrophilicity index (ω) in atomic units for the G0-precursors and dendrimer G0 at the HF/3-21G* (first row), MP2/6-311+G* (second row) and B3LYP/6-311++G** (third row) levels.

<i>Molecule</i>	<i>Energy</i>	ϵ_{HOMO}	ϵ_{LUMO}	η	ω
EDA	-188.210	-0.351	0.267	0.309	0.0028
	-189.941	-0.372	0.072	0.222	0.050
	-190.582	-0.232	-0.011	0.111	0.067
M1	-432.691	-0.352	0.210	0.281	0.0090
	-436.621	-0.385	0.059	0.222	0.060
	-437.982	-0.244	-0.023	0.111	0.080
M2	-432.697	-0.355	0.211	0.283	0.0092
	-436.627	-0.375	0.056	0.215	0.059
	-437.987	-0.247	-0.019	0.114	0.077
M3	-432.697	-0.355	0.211	0.283	0.0092
	-436.628	-0.375	0.056	0.215	0.059
	-437.986	-0.231	-0.025	0.103	0.080
M4	-432.700	-0.354	0.207	0.281	0.0097
	-436.631	-0.381	0.065	0.223	0.056
	-437.989	-0.236	-0.017	0.110	0.073
M5	-432.701	-0.356	0.221	0.288	0.0079
	-436.631	-0.378	0.063	0.221	0.056
	-437.990	-0.239	-0.021	0.109	0.077
D1	-565.030	-0.336	0.210	0.273	0.0073
	-570.184	-0.365	0.058	0.211	0.056
	571.987	-0.225	-0.021	0.102	0.074
D2	-565.035	-0.338	0.203	0.271	0.0085
	-570.191	-0.369	0.061	0.215	0.055
	-571.992	-0.227	-0.019	0.104	0.072
T1	-941.852	-0.329	0.206	0.268	0.0070
	-950.434	-0.354	0.050	0.202	0.057
	-953.390	-0.214	-0.026	0.094	0.077
T1T1	-1318.630	-0.328	0.185	0.256	0.0099
	-1330.680	-0.343	0.056	0.199	0.052
	-1334.798	-0.209	-0.024	0.092	0.073
T1T2	-1318.639	-0.327	0.187	0.257	0.0095
	-1330.690	-0.341	0.059	0.200	0.050
	-1334.806	-0.207	-0.023	0.092	0.072

G0	-1695.442	-0.315	0.172	0.244	0.0105
	-1710.928	-0.334	0.039	0.186	0.058
	-1716.198	-0.203	-0.032	0.086	0.080

From Table 3 and Figures 5 and 6, we may note that hardness values show a clear decreasing tendency as the molecules are sizely bigger for the three levels of theory, which means that as the size of the precursor increases toward G0 the polarizability of the molecules increases, i.e., their corresponding densities tend to be more delocalized and hence more reactive in chemical terms with the G0 dendrimer being the most reactive. It is also interesting to note that hardness values are smaller as correlation increases, which is in agreement with the energy trends observed from Table 3 in that the B3LYP energy values are negatively larger than MP2 ones and these in turn more negative than the HF values. On the other hand, the electrophilicity behavior may be analyzed from Figure 6 which roughly indicates a tendency to acquire electronic charge, i.e., as the size of the precursors increase they are more polarizable and hence more reactive, except for the tetramer precursors (TT1 and TT2) which show smaller values for correlated methods as compared with the rest. It is also worth mentioning that as correlation increases from HF values to B3LYP ones, the electrophilicity values increase, which agrees with Eq. 8 in that electrophilicity is inversely proportional to the hardness, and this is what we observed from Figures 5 and 6.

Observations above are in agreement with the results for the dipole moment components in that higher generation dendrimers possess more polarized molecular densities. Further, it is known that less compact molecules are more polarizable, with low hardness values and hence more reactive, and this is indeed the case when comparing the softness values depicted in Figure 7 with the size of the molecules which can be estimated through the radius of gyration R_g shown in Figure 2.

1
2
3
4
5
6
7
8
9
10
11
12
13
14
15
16
17
18
19
20
21
22
23
24
25
26
27
28
29
30
31
32
33
34
35
36
37
38
39
40
41
42
43
44
45
46
47
48
49
50
51
52
53
54
55
56
57
58
59
60

Next, we examine the Shannon information entropies in real space, Eqs (9) and (10). In Fig 8 the entropy sum, S_r+S_p , and the energy (Table 3) are depicted for the PAMAM G0-precursors and dendrimer G0. It is apparent from Figure 8 that the total entropy follows the opposite behavior as the energy, i.e., as the size of the molecules increases so does the entropy sum. It is also interesting to note that the total entropy distinguishes the different polymeric structures in that isoelectronic systems possess the same entropy value and so does the energy.

Moreover, a similar behavior is shown in Figure 9, where the Shannon entropies in position and momentum spaces are depicted at the HF/3-21G* level. Whereas the momentum space entropies are fairly constant for all systems, the position entropy reveals more structure in that as the size of the precursors increases there is a clear trend to get more delocalized densities, and hence less compact structures which tend to be more polarizable as discussed above (see Fig 7). This observation is in fair agreement with the dense core model as a growing model for dendrimers. In contrast, the momentum space entropy does not show significant changes among the different structures as the dispersion of the values for this measure is very small as compared to the position entropy.

Finally, we investigate the information entropies in Hilbert space, Eqs. (11) and (12), in connection with the growing behavior of PAMAM dendrimers. It is important to mention that whereas Shannon entropies in real space represent costly and time consuming calculations, Hilbert space entropies do not pose additional computational efforts as to the theoretic-information analyses concerns, of course the obtaining of the wave functions and the NAP values represent a challenge for electronic structure calculations and the present computation capabilities available to us. Thus, we have performed the necessary calculations at the HF/3-21G* level for analyzing additional structures, the trimer conformations T2 through T4, along with G1 through G3 dendrimers (G1 with 228 atoms, G2 with 516 atoms, and G3 with 1092 atoms). In Figure 10 we

1
2
3
4
5
6
7
8
9
10
11
12
13
14
15
16
17
18
19
20
21
22
23
24
25
26
27
28
29
30
31
32
33
34
35
36
37
38
39
40
41
42
43
44
45
46
47
48
49
50
51
52
53
54
55
56
57
58
59
60

have depicted the Shannon entropy $H(A)$ for all the PAMAM G0-precursors along with the G0 through G3 dendrimers. This measure allows to determine the global information content of the systems and consequently we may observe from Figure 10 that $H(A)$ shows an increasing behavior as the size of the precursors and dendrimers increases. This again supports the above discussed dense-core model of dendrimers as bigger molecules show more uncertainty in Hilbert space, which corresponds to less compact densities in real space and hence to more delocalized electronic distributions.

Furthermore, in Figure 11 we have plotted the Kullback-Leibler relative entropy in Hilbert space $H(A|B)$, along with the total energy values for all dendrimer precursors and dendrimers G0 through G3, calculated at the HF/3-21G* level. The Kullback-Leibler measure represents a distance from a reference probability distribution, which in this case we have set for the EDA molecule (which is embedded in all the structures). We may observe from the Figure 11 that as the molecules depart from EDA the Hilbert information distance increases in a monotonically fashion which reflects the core-dense growing behavior of dendrimers by simply measuring the information distance between EDA and the increasingly bigger molecules. Assuming that dendrimers follow a hollow-core model of growth and hence a dense shell model, the $H(A|B)$ trend would have been just the opposite.

Interestingly, Figures 10 and 11 show the ability of these quantum measures to reveal and corroborate two simple facts already discussed in the literature [52]: (i) the validity of the core-dense model witnessed by the mutual von Neumann entropy of the marginal type, as the $H(A|B)$ Hilbert distance increases monotonically in going from the precursors to higher generation dendrimers, and (ii) the global information content of the systems, $H(A)$, which increases monotonically as one would expect from a thermodynamic point of view (entropy). A particular feature that may be noted from Figure 9 is the capacity of $H(A)$ of measuring the atomic and electronic content of the

1
2
3
4
5 systems, regardless of its conformational structure, which is characteristic of the energy. The
6
7 relevancy of these results might be assessed by considering that the equivalent information in real
8
9 space implied the calculation of position and momentum space entropies of the Shannon type
10
11 which, taking into account the size of the systems (1023 atoms for G3 dendrimer), represents
12
13 indeed a formidable task to compute, even by taking into consideration that the integration
14
15 quadratures were guided by promolecular grids [53]. Ongoing research is being undertaken in our
16
17 laboratories to extend the study to higher generation PAMAM dendrimers mainly on the side of the
18
19 Hilbert space framework.
20
21
22
23
24
25

26 CONCLUSION

27
28
29
30 Throughout this investigation we have employed selected polymer science parameters along with
31
32 chemical reactivity descriptors which show numerical evidence supporting the dense-core model of
33
34 dendrimers Besides, we have corroborated through higher level calculations which take into account
35
36 the effects of electron correlation, that the behavior observed at the HF level depicts basically the
37
38 same physical and chemical features. These results allow us to perform a more demanding
39
40 computational study at the HF level in order to study the growing behavior of dendrimer precursors
41
42 from a theoretic-information perspective. Thus, it was shown that Shannon entropies defined in
43
44 real space, S_r and S_p , as well as the information measures in Hilbert space, $H(A)$ and $H(A|B)$, are
45
46 capable of revealing the dense core growing behavior of dendrimers, by showing that bigger
47
48 molecules possess more delocalized electronic distributions in such a way to span their molecular
49
50 distributions as the molecular size increases.
51
52
53
54
55
56
57
58
59
60

1
2
3
4
5
6
7
8
9
10
11
12
13
14
15
16
17
18
19
20
21
22
23
24
25
26
27
28
29
30
31
32

To the best of our knowledge the results presented in this work represent benchmark calculations for ES *ab initio* studies at three different levels of theory and with the inclusion of electron correlation. Thus, from the present study we may conclude that it is feasible to employ ES *ab initio* methods to analyze PAMAM-EDA dendrimers, at least for low levels of theory, revealing the same basic features of more thorough studies of Monte Carlo and atomistic Molecular Dynamics type [19]. It is also worth mentioning that chemical reactivity indexes like the ones employed here may provide deeper insights into the structural properties and growing behavior of dendrimers. An important result of this work is the application of Hilbert space information measures to PAMAM-dendrimers, which were shown to reveal the same basic features of equivalent information measures in real space, which require much more expensive computations though [54].

33 ACKNOWLEDGMENTS

34
35
36
37
38
39
40
41
42
43
44
45
46
47
48
49
50
51
52
53
54
55
56
57
58
59
60

We wish to thank José María Pérez-Jordá and Miroslav Kohout for kindly providing with their numerical codes. R.O.E. wishes to thank Juan Carlos Angulo and Jesús Sánchez-Dehesa for their kind hospitality during his sabbatical stay on the Departamento de Física Atómica, Molecular y Nuclear at the Universidad de Granada, Spain. We acknowledge financial support from CONACyT (México) through grant 082266 and from PROMEP-SEP (México). We acknowledge financial support through mexican grants 08226 CONACyT, PIFI 3.3 PROMEP-SEP and Spanish grants MICINN projects FIS-2008-02380, FIS-2005-06237 (J.A.), FQM-1735, P05-FQM-00481 and P06-FQM-2445 of Junta de Andalucía. J.C. A. and J.A. belong to the Andalusian research group FQM-0207. E.M.C. wishes to thank CONACyT (México) for a PhD fellowship. Allocation of supercomputing time from the Departamento de Supercómputo at

DGSCA-UNAM, the Sección de Supercomputacion at CSIRC-Universidad de Granada, and the Laboratorio de Supercómputo y Visualización at UAM is gratefully acknowledged.

REFERENCES

- [1] D. A. Tomalia, H. Baker, J. Dewald, M. Hall, G. Kallos, S. Martin, J. Roeck, J. Ryder, P. Smith, A New Class of Polymers: Starburst Dendritic Macromolecules *Polym. J.* 17, (1985) 117-132
- [2] a) G. R. Newkome, C. N. Moorefield, F. Vögtle, *Dendritic molecules: Concepts, Synthesis, Perspectives*, Wiley-VCH, Weinheim, 1996; b) Fréchet J M J, Tomalia D A. , editors. *Dendrimers and Other Dendritic Polymers*. Chichester, U.K.: Wiley; 2001.
- [3] Hecht, S; Fréchet, J M, *Dendritic Encapsulation of Function: Applying Nature's Site Isolation Principle from Biomimetics to Materials Science*, *J. Angew Chem Int Ed Engl.* 2001;40:74–91
- [4] H. M. Janssen, E. W. Meijer, In *Synthesis of Polymers: Materials Science and Technology Series*; A. D. Schüter, Ed.; R. W. Cahn, P. Haasen, E. J. Kramer,, series Eds.; Wiley-VCH: Weinheim, 1999; p 403.
- [5] a) M. Fischer, F. Vögtle *Dendrimers: From Design to Application - A Progress Report*, *Angew. Chem., Int. Ed.*, 38, (1999) 884-905; b) F. Zeng;; S. C. Zimmerman, *Dendrimers in Supramolecular Chemistry: From Molecular Recognition to Self-Assembly* *Chem. Rev.*, 97, (1997)1681-1712; c) O. A. Matthews, A. N. Shipway, J. F. Stoddart, *Dendrimers: Branching out from curiosities into new technologies* *Prog. Polym. Sci.* 23 (1998), 1-56; d) P. Holister, C. Roman-Vas, T. Harper, *Dendrimers, Technology White Papers*", Vol 6, (2003), 1-15.
- [6] a) D. A. Tomalia, A. M. Naylor;; W. A., Goddard III, *Starburst Dendrimers: Molecular-Level Control of Size, Shape, Surface Chemistry, Topology, and Flexibility from Atoms to Macroscopic Matter* *Angew. Chem., Int. Ed. Engl.*, 29 (1990)138-175; b) D. A. Tomalia, B. Huang, D. R. Swanson, H. M. Brothers, II, J. W. Klimash, *Structure control within poly(amidoamine) dendrimers: size, shape and regio-chemical mimicry of globular proteins* *Tetrahedron* 59, (2003) 3799-3813; c) H.-F. Chow, T. K.-K. Mong, Y.-H. Chan, C. H. Cheng *Tetrahedron* 59 (2003), 3915; d) F. Diederich, B. Felber,. *Proc. Natl. Acad. Sci. U.S.A.*, 99, (2002) 4779; e) L. Liu, R. Breslow, *J. Am. Chem. Soc.* 125, (2003)12110.

- 1
2
3
4
5
6 [7] F. Zeng, S. C. Zimmerman, *Chem. Rev.*, 97, (1997)1681.
- 7 [8] a) F. Vögtle, S. Gestermann, R. Hesse, H. Schwierz, Windisch, B. *Prog. Polym. Sci.*, 25,
8 (2000) 987; b) A. Adronov, J. M. Fréchet, *J. Chem. Commun.* 18, (2000) 1701; c) A. W.
9 Freeman, S. C. Koene, P. R. L. Malenfant, M. E. Thompson, J. M. J. Fréchet, *J. Am. Chem.*
10 *Soc.* 122, (2000) 12385; d) V. Balzani, P. Ceroni, S. Gestermann, C. Kauffmann, M.
11 Gorkab, F. Vögtle, *Chem. Commun.* 10, (2000) 853.
- 12 [9] a) J. M. Fréchet, Dendrimers and supramolecular chemistry, *J. Proc. Natl. U.S.A.* 99, (2002)
13 4782-4787; S. C. Zimmerman, V. Zeng, *Science* 271, (1996)1095; b) J. F. G. A. Jansen, E.
14 W. de Brabander- *Science* 266, (1994) 1226.
- 15 [10] S. Jockush, J. Ramirez, K. Sanghvi, R. Nociti, N. J. Turro, D. A. Tomalia, Comparison of
16 Nitrogen Core and Ethylenediamine Core Starburst Dendrimers through Photochemical and
17 Spectroscopic Probes, *Macromolecules* 32, (1999) 4419-4423.
- 18 [11] a) M. Ballauff, Dendrimers III: Design, Dimension, Function:, *Top. Curr. Chem.* 212,
19 (2001)177 – 194; b) D. Pötschke, M. Ballauff, Structure of Dendrimers in Solution as Probed
20 by Scattering Experiments, in *Structure and Dynamics of Polymer and Colloidal Systems*
21 (Eds.: R. Borsali, R. Pecora), Kluwer, Dordrecht, 2002; c) S. Hecht, Functionalizing the
22 interior of dendrimers: Synthetic challenges and applications *J. Polym. Sci. Part A*, 41 (2003)
23 1047 – 1058; d) G. R. Newkome, C. Moorefield, F. Vogtle, *Dendrimers and Dendrons*,
24 Wiley-VCH, New York, 2001
- 25 [12] P. G. de Gennes, H. Hervet, Statistics of starburst polymers, *J. Phys. Lett.* 44, (1983) L351-
26 L360.
- 27 [13] S. F. Edwards, The statistical mechanics of polymers with excluded volume, *Proc. Phys. Soc.*
28 London 85, (1965) 613 – 624.
- 29 [14] R. L. Lescanec, M. Muthukumar, Configurational characteristics and scaling behavior of
30 starburst molecules: a computational study, *Macromolecules* 23, (1990) 2280 – 2288.
- 31 [15] D. Boris, M. Rubinstein, A Self-Consistent Mean Field Model of a Starburst Dendrimer:
32 Dense Core vs Dense Shell, *Macromolecules* 1996, 29, 7251 – 7260 ; T. C. Zook, G. Pickett,
33 Hollow-Core Dendrimers Revisited *Phys. Rev. Lett.* 90 (2003)105502.
- 34 [16] R. La Ferla, Conformations and dynamics of dendrimers and cascade macromolecules *J.*
35 *Chem. Phys.* 1997, 106, 688 – 700; F. Ganazzoli, R. La Ferla, G. Terragni, Conformational
36 Properties and Intrinsic Viscosity of Dendrimers under Excluded-Volume Conditions
37 *Macromolecules* 33, (2000) 6611 – 6620 ; F. Ganazzoli, Conformations and dynamics of
38
39
40
41
42
43
44
45
46
47
48
49
50
51
52
53
54
55
56
57
58
59
60

- stars and dendrimers: the Gaussian Self-Consistent approach, *Condens. Matter Phys.* 5, (2002) 37 -71.
- [17] E. G. Timoshenko, Yu. A. Kuznetsov, R. Connolly, Conformations of dendrimers in dilute solution, *J. Chem. Phys.* 117, (2002) 9050 – 9062.
- [18] M. P. Allen, D. J. Tildesley, *Computer Simulation of Liquids*, Clarendon, Oxford, 1987; D. Frenkel, B. Smit, *Understanding Molecular Simulation*, Academic Press, San Diego, 1996.
- [19] P.K. Maiti, T Cagin, G. Wang, W.A. Goddard III, Structure of PAMAM Dendrimers: Generations 1 through 11, *Macromolecules* 37, (2004) 6236-6254
- [20] F. Tarazona-Vasquez, P. B. Balbuena, plexation of the Lowest Generation Poly(amidoamine)-NH₂ Dendrimers with Metal Ions, Metal Atoms, and Cu(II) Hydrates: An ab Initio Study, *J. Phys. Chem. B* 108, (2004)15992-16001; F. Tarazona-Vasquez, P. B. Balbuena, Ab Initio Study of the Lowest Energy Conformers and IR Spectra of Poly(amidoamine)-G0 Dendrimers *J. Phys. Chem. B* 108, (2004) 15982-15991; Ch. Lin, K. Wu, R. Sa, Ch. Mang, P. Liu, B. Zhuang, Density functional theory studies on the potential energy surface and hyperpolarizability of polyamidoamide dendrimer, *Chem Phys Lett* 363 (2002) 343–348; S. K. Avinash, R. D. Nilesh P. G. Shridhar, Hartree–Fock and density functional studies on the structure and vibrational frequencies of quinoxalines—the building blocks for dendrimers, *J. Mol. Struct. Theochem* 589-590, (2002) 301-309
- [21] a) R. F. W. Bader, *An Introduction to the Structure of Atoms and Molecules*, Toronto, Clarke, 1970; b) R. F. W. Bader, *Atoms in Molecules*, New York, Oxford, 1994; c) P. Ayers, Atoms in molecules, an axiomatic approach. I. Maximum transferability, *J. Chem. Phys.* 113 (2000) 10886-10898; d) R. F. W. Bader, T. T. Nguyen-Dang, *Quantum Theory of Atoms in Molecules: Dalton Revisited*, *Adv. Quantum Chem.* 14 (1981) 63-124; e) A. Cedillo, P. K. Chattaraj, and R. G. Parr, Atoms-in-molecules partitioning of a molecular density, *Int. J. Quantum Chem.* 77 (2000) 403-407; f) F. L. Hirshfeld, Bonded-atom fragments for describing molecular charge densities, *Theor. Chim. Acta* 44 (1977) 129-138; g) R. G. Parr, R. A. Donnelly, M. Levy, and W. E. Palke, Electronegativity: The density functional viewpoint, *J. Chem. Phys.* 68 (1978) 3801-3807; h) R. G. Parr, Remarks on the concept of an atom in a molecule and on charge transfer between atoms on molecule formation, *Int. J. Quantum Chem.* 26 (1984) 687-692; i) J. Rychlewski, R. G. Parr, The atom in a molecule: A wave function approach, *J. Chem. Phys.* 84 (1986) 1696-1703; j) L. Li, R. G. Parr, The atom in a molecule: A density matrix approach, *J. Chem. Phys.* 84 (1986) 1704-1711

- 1
2
3
4
5
6 [22] J. Lin, Divergence measures based on the Shannon entropy, IEEE Trans. On Inf. Theory,
7 37 (1991) 145-151
8
- 9 [23] a) W. Moffitt, Atoms in Molecules and Crystals , Proc. R. Soc. London, Ser. A 210 (1951)
10 245-268; b) R. S. Mulliken, Electronic Structures of Molecules XI. Electroaffinity, Molecular
11 Orbitals and Dipole Moments, J. Chem. Phys. 3 (1935) 573-585; c) R. S. Mulliken,
12 Electronic Population Analysis on LCAO—MO Molecular Wave Functions. I, J. Chem.
13 Phys. 23 (1955) 1833-1840
14
15
16
17
- 18 [24] A.E. Reed, R.B. Weinstock, F. Weinhold, Natural population analysis, J. Chem. Phys. 83
19 (1985) 735-746
20
- 21 [25] G. Bruhn, E. R. Davidson, I. Mayer, A. E. Clark, Löwdin population analysis with and
22 without rotational invariance, Int. J. Quantum Chem. 106 (2006) 2065-2072
23
- 24 [26] P. O. Löwdin., Quantum Theory of Many-Particle Systems. I. Physical Interpretations by
25 Means of Density Matrices, Natural Spin-Orbitals, and Convergence Problems in the
26 Method of Configurational Interaction, Phys. Rev. 97 (1955) 1474-1489
27
28
- 29 [27] E. Carrera, N. Flores-Gallegos and R.O. Esquivel , Natural Atomic Probabilities in
30 Quantum Information Theory , J. Comp. App. Math. (in press)
31
32
33
34
- 35 [28] a) Sears, S. B.; Parr, R. G.; Dinur, U., On the quantum-mechanical kinetic energy as a
36 measure of the information in a distribution, Isr. J. Chem. 1980, 19, 165-173; b) Koga, T.;
37 Morita, M., Maximum-entropy inference and momentum density approach, J. Chem. Phys.
38 1983, 79, 1933-1938; c) S. R. Gadre, S. B. Sears, S. J. Chakravorty, and R. D. Bendale, Some
39 novel characteristics of atomic information entropies, Phys. Rev. A 1985, 32, 2602-2607; d)
40 Angulo, J. C.; Dehesa, J. S., Tight rigorous bounds to atomic information entropies , J.
41 Chem. Phys. 1992, 97, 6485-6495; e) Antolín, J.; Zarzo, A., Angulo, J. C. , Upper and lower
42 bounds on the radial electron density in atoms, Phys. Rev. A 1993, 48, 4149-4155; f)
43 Ramirez, J.C.; Perez, J.M.H.; Sagar, R.P.; Esquivel, R.O.; Ho, M.; Smith Jr., V. H., Amount
44 of information present in the one-particle density matrix and the charge density, Phys. Rev.
45 A 1998, 58, 3507-3515; g) Nalewajski, R. F.; Parr, R. G., Information Theory
46 Thermodynamics of Molecules and Their Hirshfeld Fragments, J. Phys. Chem. A, 2001, 105,
47 7391-7400; h) Nagy, A., Fisher information in density functional theory, J. Chem. Phys. 2003,
48 119, 9401-9405; i) Romera E.; Dehesa, J. S., The Fisher–Shannon information plane, an
49 electron correlation tool, J. Chem. Phys. 2004, 120, 8906-8912; j) Sen, K. D., Characteristic
50
51
52
53
54
55
56
57
58
59
60

- 1
2
3
4
5
6 features of Shannon information entropy of confined atoms, *J. Chem. Phys.* 2005, 123,
7 074110(1-9); k) Parr, R. G.; Nalewajski, R. F.; Ayers, P. W., What Is an Atom in a Molecule?,
8 *J. Phys. Chem. A* 2005, 109, 3957-3959; l) Guevara, N. L.; Sagar, R. P.; Esquivel, R. O.,
9 Local correlation measures in atomic systems, *J. Chem. Phys.* 2005, 122, 084101-1—084101-
10 8; m) Nagy, A., Fisher information in a two-electron entangled artificial atom, *Chem. Phys.*
11 *Lett.* 2006, 425, 154-156; n) Ayers, W., Density bifunctional theory using the mass density
12 and the charge density, *Theor. Chem. Acc.* 2006, 115, 253-256; o) Liu, S. J., On the
13 relationship between densities of Shannon entropy and Fisher information for atoms and
14 molecules, *Chem. Phys.* 2007, 126, 191107-1-91107-3.
- [29] G. Rudnick, G. Gaspari, The aspherity of random walks, *J. Phys. A* 4, (1986) L191-194.
- [30] R. G. Parr, R. G Pearson, Absolute hardness: companion parameter to absolute
23 electronegativity, *J Am Chem Soc* 105, (1983) 7512-7516; Parr, R. G.; Yang, W. "Density-
24 Functional Theory of Atoms and Molecules", Oxford University Press: New York, 1989
25
26
27
28
29
- [31] Koopmans, T. A., Ueber die Zuordnung von Wellenfunktionen und Eigenwerten zu den
30 einzelnen Elektronen eines Atoms, *Physica* 1933, 1, 104-113; Janak, J. F., Proof that $\partial E /$
31 $\partial n_i = \epsilon$ in density-functional theory, *Phys. Rev B* 1978, 18, 7165-7168.
32
33
34
35
36
- [32] Ghanty, T. K.; Ghosh, S. K., Correlation between hardness, polarizability, and size of atoms,
37 molecules, and clusters, *J. Phys. Chem.* 1993, 97, 4951-4953; Roy, R.; Chandra, A.K.; Pal, S.,
38 Correlation of Polarizability, Hardness, and Electronegativity: Polyatomic Molecules, *J. Phys.*
39 *Chem.*, 1994, 98, 10447-10450; Hati, S.; Datta, D., Hardness and Electric Dipole
40 Polarizability. Atoms and Clusters, *J. Phys. Chem.* 1994, 98, 10451-10454; Simon-Manso, Y.;
41 Fuentealba, P., On the Density Functional Relationship between Static Dipole Polarizability
42 and Global Softness, *J. Phys. Chem. A* 1998, 102, 2029-2032.
43
44
45
46
47
48
- [33] Chattaraj, P.K.; Sarkar, U.; Roy, D. R. , Electrophilicity Index, *Chem Rev* 2006, 106, 2065-
49 2091.
50
51
- [34] Pearson, R. G., Hard and Soft Acids and Bases. *J. Am. Chem. Soc.* 1963, 85, 3533; Pearson,
52 R. G., Hard and Soft Acids and Bases; Downen, Hutchinson and Ross: Stroudsburg, 1973.;
53 Pearson, R. G., Chemical Hardness; Wiley-VCH; New York, 1997.
54
55
56
- [35] Parr, R. G.; Szentpály, L. V.; Liu, S., Electrophilicity Index, *J Am Chem Soc* 1999, 121,
57 1922-1924.
58
59
60

- 1
2
3
4
5
6 [36] Shannon, C.E., A mathematical theory of communication, Bell Syst. Tech. J. 1948, 27, 379-
7 423
8
9 [37] Bialynicky-Birula, I.; Mycielski, Uncertainty relations for information entropy in wave
10 mechanics, J. Commun. Math. Phys. 1975, 44, 129-132.
11
12
13
14 [38] P.O. Lowdin, On the orthogonality problem, Adv. Quantum Chem. 5, (1970) 185
15
16 [39] A.E. Reed and F. Weinhold, Natural bond orbital analysis of near-Hartree-Fock water
17 dimmer, J. Chem. Phys. 78, (1983) 4066-4073
18
19 [40] E.R. Davidson, Electronic Population Analysis of Molecular Wavefunctions, J. Chem. Phys.
20 46, (1967) 3320-3324
21
22 [41] a) A.E. Reed, R.B. Weinstock, F. Weinhold, Natural population analysis J. Chem. Phys. 83,
23 (1985) 735-746
24
25
26 [42] N. Flores-Gallegos, R. O. Esquivel, von Neumann Entropies Analysis in Hilbert Space for
27 the Dissociation Processes of Homonuclear and Heteronuclear Diatomic Molecules, J. Mex.
28 Chem. Soc. 2008, 52(1), 19-30
29
30
31 [43] A. Wehrl, General properties of entropy, Rev. Mod. Phys. 50, (1978) 221-260; V. Vedral,
32 The role of relative entropy in quantum information theory, Rev Mod. Phys. 74, (2002)197-
33 234
34
35
36 [44] C. E. Shannon, W. Weaver 1949, The Mathematical Theory of Communication
37 (University of Illinois, Urbana, IL).
38
39 [45] Kullback, S.; and Leibler R. A., On Information and Sufficiency, Ann. Math. Stat. 1951, 22,
40 79-86.
41
42
43 [46] E. J. Bylaska, W. A. de Jong, K. Kowalski, T. P. Straatsma, M. Valiev, D. Wang, E. Apra, T.
44 L. Windus, S. Hirata, M. T. Hackler, Y. Zhao, P.-D. Fan, R. J. Harrison, M. Dupuis, D. M.
45 A. Smith, J. Nieplocha, V. Tipparaju, M. Krishnan, A. A. Auer, M. Nooijen, E. Brown, G.
46 Cisneros, G. I. Fann, H. Fruchtl, J. Garza, K. Hirao, R. Kendall, J. A. Nichols, K.
47 Tsemekhman, K. Wolinski, J. Anchell, D. Bernholdt, P. Borowski, T. Clark, D. Clerc, H.
48 Dachsel, M. Deegan, K. Dylla, D. Elwood, E. Glendening, M. Gutowski, A. Hess, J. Jaffe, B.
49 Johnson, J. Ju, R. Kobayashi, R. Kutteh, Z. Lin, R. Littlefield, X. Long, B. Meng, T.
50 Nakajima, S. Niu, L. Pollack, M. Rosing, G. Sandrone, M. Stave, H. Taylor, G. Thomas, J.
51 van Lenthe, A. Wong, and Z. Zhang, "NWChem, A Computational Chemistry Package for
52
53
54
55
56
57
58
59
60

- 1
2
3
4
5
6
7
8
9
10
11
12
13
14
15
16
17
18
19
20
21
22
23
24
25
26
27
28
29
30
31
32
33
34
35
36
37
38
39
40
41
42
43
44
45
46
47
48
49
50
51
52
53
54
55
56
57
58
59
60
- Parallel Computers, Version 5.0" (2006), Pacific Northwest National Laboratory, Richland, Washington 99352-0999, USA.
- [47] Gaussian 03, Revision D.01, M. J. Frisch, G. W. Trucks, H. B. Schlegel, G. E. Scuseria, M. A. Robb, J. R. Cheeseman, J. A. Montgomery Jr., T. Vreven, K. N. Kudin, J. C. Burant, J. M. Millam, S. S. Iyengar, J. Tomasi, V. Barone, B. Mennucci, M. Cossi, G. Scalmani, N. Rega, G. A. Petersson, H. Nakatsuji, M. Hada, M. Ehara,; K. Toyota, R. Fukuda, J. Hasegawa, M. Ishida, T. Nakajima, Y. Honda, O. Kitao, H. Nakai, M. Klene, X. Li, J. E. Knox, H. P. Hratchian, J. B. Cross, V. Bakken, C. Adamo, J. Jaramillo, R. Gomperts, R. E. Stratmann, O. Yazyev, A. J. Austin, R. Cammi, C. Pomelli, J. W. Ochterski, P. Y. Ayala, K. Morokuma, G. A. Voth, P. Salvador, J. J. Dannenberg, V. G. Zakrzewski, S. Dapprich, A. D. Daniels, M. C. Strain, O. Farkas, D. K. Malick, A. D. Rabuck, K. Raghavachari, J. B. Foresman, J. V. Ortiz, Q. Cui, A. G. Baboul, S. Clifford, J. Cioslowski, B. B. Stefanov, G. Liu, A. Liashenko, P. Piskorz, I. Komaromi, R. L. Martin, D. J. Fox, T. Keith, M. A. Al-Laham, C. Y. Peng, A. Nanayakkara, M. Challacombe, P. M. W. Gill, B. Johnson, W. Chen, M. W. Wong, C. Gonzalez, J. A. Pople, 2004, Gaussian, Inc., Wallingford CT)
- [48] The geometric parameters of dendrimers G0 through G3 were obtained from P.K. Maiti (see Ref. 19)
- [49] NBO 5.0. Glendening E. D. Badenhoop J, K. Reed A. E. Carpenter J. E. Bohmann J. A. Morales C. M. and Weinhold F. Theoretical Chemistry Institute 2001, University of Wisconsin, Madison
- [50] Pérez-Jordá, J. M.; San-Fabián, E. , A simple, efficient and more reliable scheme for automatic numerical integration, *Comput Phys Commun*, 1993, 77, 46–56; Pérez-Jordá, J. M.; Becke, A. D.; San-Fabián, E., Automatic numerical integration techniques for polyatomic molecules, *J Chem Phys* 1994, 100, 6520–6534.
- [51] Kohout M. program DGRID, version 4.2. 2007
- [52] M. Ballauff , C. N. Likos, *Dendrimers in Solution: Insight from Theory and Simulation*, *Angew. Chem. Int. Ed.* 43, (2004) 2998 – 3020
- [53] The grids obtained by use of AUTOM (Ref. 50) were obtained by using promolecular densities as generating kernel functions. For dendrimers G0 through G3, with a relative tolerance of 1×10^{-5} , the grid consists of 4.3 M (million points), 10.6M, 34M, and 79.5M, respectively. Roughly, each point takes 1 sec in a high performance supercomputer (per

processor). So that, it is highly desirable to employ large array supercomputers to accomplish this kind of studies in a reasonable time.

FIGURE CAPTIONS

Figure 1. Dipole moment components in Debyes for the PAMAM polymeric precursors and the G0 dendrimer structure at the HF/3-21G* level. (μ_x : empty boxes, μ_y : empty circles and μ_z : empty triangles).

Figure 2. The radius of gyration R_g as a function of generation for the G0-precursors and the G0-PAMAM dendrimer calculated at the HF/3-21G* level of theory.

Figure 3. Moment of inertia aspect ratios I_z/I_x (empty circles), I_z/I_y (solid boxes) for the G0-precursors and the G0-PAMAM dendrimer calculated at the HF/3-21G* level of theory.

Figure 4. The asphericity parameter δ as a function of generation for the G0-precursors and the G0-PAMAM dendrimer calculated at the HF/3-21G* level of theory.

Figure 5. The hardness η values for the G0-precursors and G0 dendrimer at the HF(/3-21G* (solid triangles), the MP2/6-311+G* (solid circles) and at the B3LYP/6-311++G** (solid boxes) levels of theory.

1
2
3
4
5
6
7
8
9
10
11
12
13
14
15
16
17
18
19
20
21
22
23
24
25
26
27
28
29
30
31
32
33
34
35
36
37
38
39
40
41
42
43
44
45
46
47
48
49
50
51
52
53
54
55
56
57
58
59
60

Figure 6. The electrophilicity index for the G0-precursors and the G0 dendrimer at the HF/3-21G* (solid triangles), the MP2/6-311+G* (solid circles), and at the B3LYP/6-311++G** (solid boxes) levels of theory.

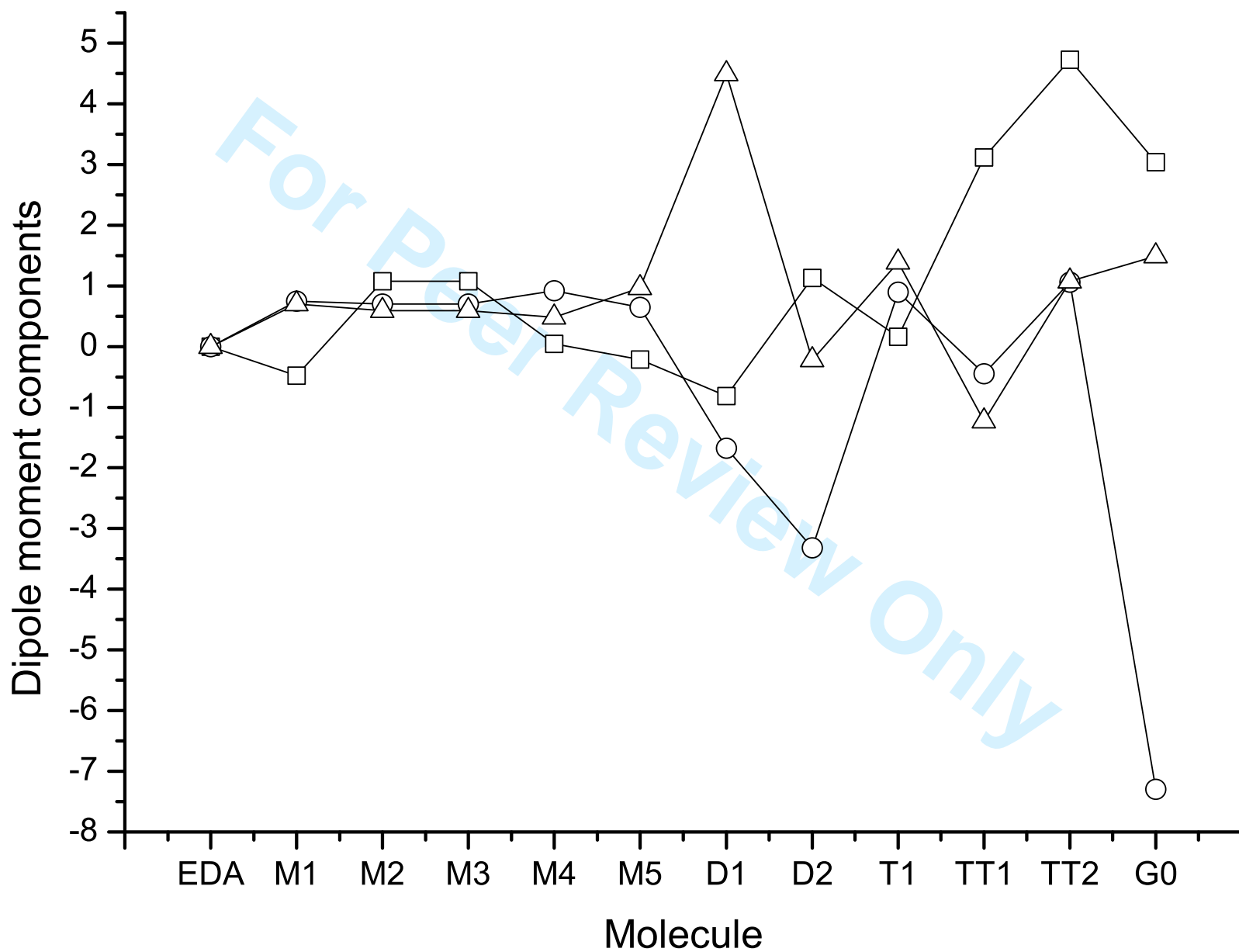
Figure 7. The softness “S” values for the G0-precursors and the G0 dendrimer at the HF/3-21G* (solid triangles), the MP2/6-311+G* (solid circles), and at the B3LYP/6-311++G** (solid boxes) levels of theory.

Figure 8. Shannon entropy sum (empty circles) and the total energies in a.u. (empty triangles) for the PAMAM polymeric precursors at the HF/3-21G* level.

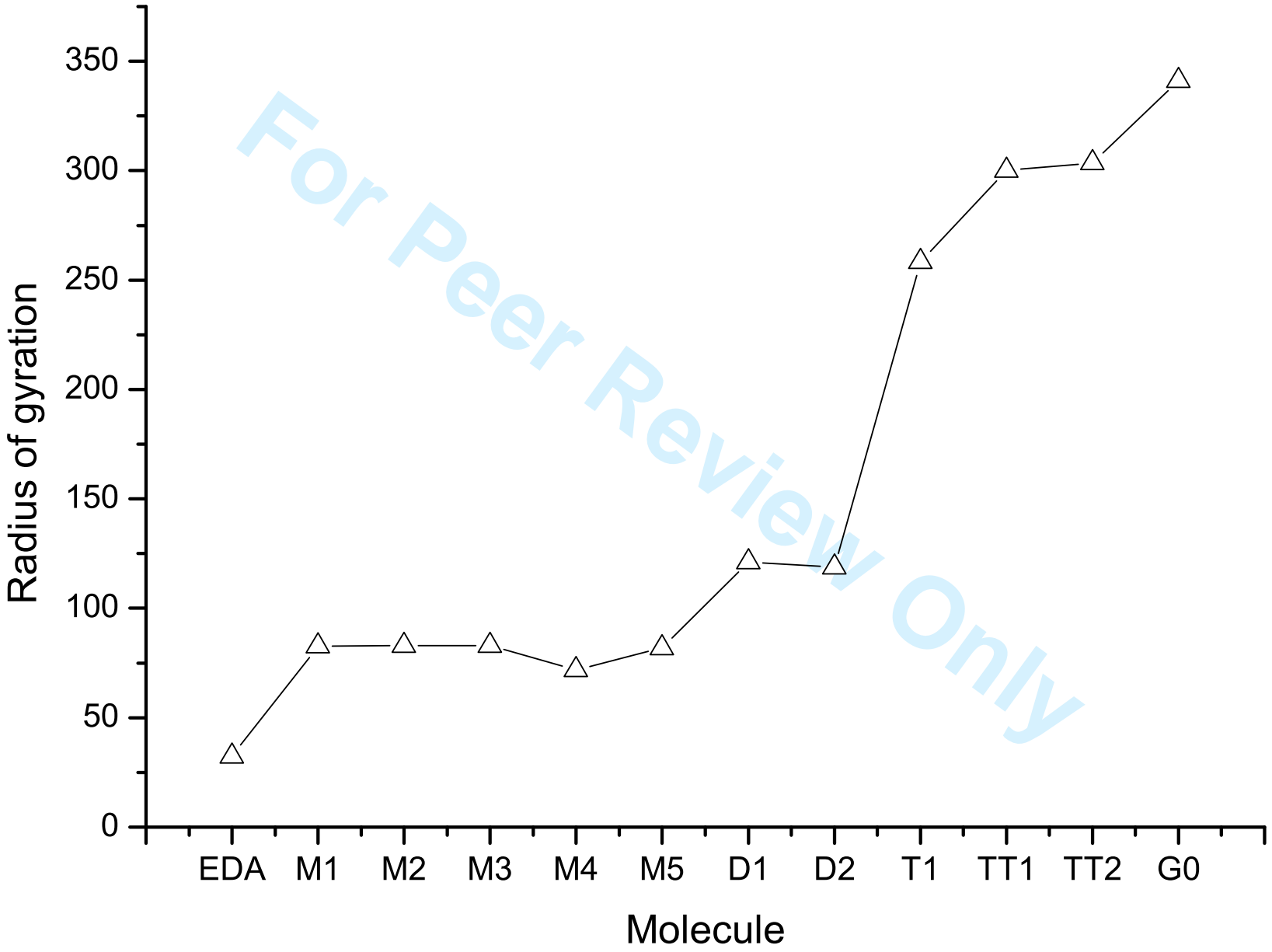
Figure 9. Shannon entropies in position (triangles) and momentum (stars) spaces (Eqs. 9 and 10) for the G0-precursors and the G0 dendrimer at the HF/3-21G* level.

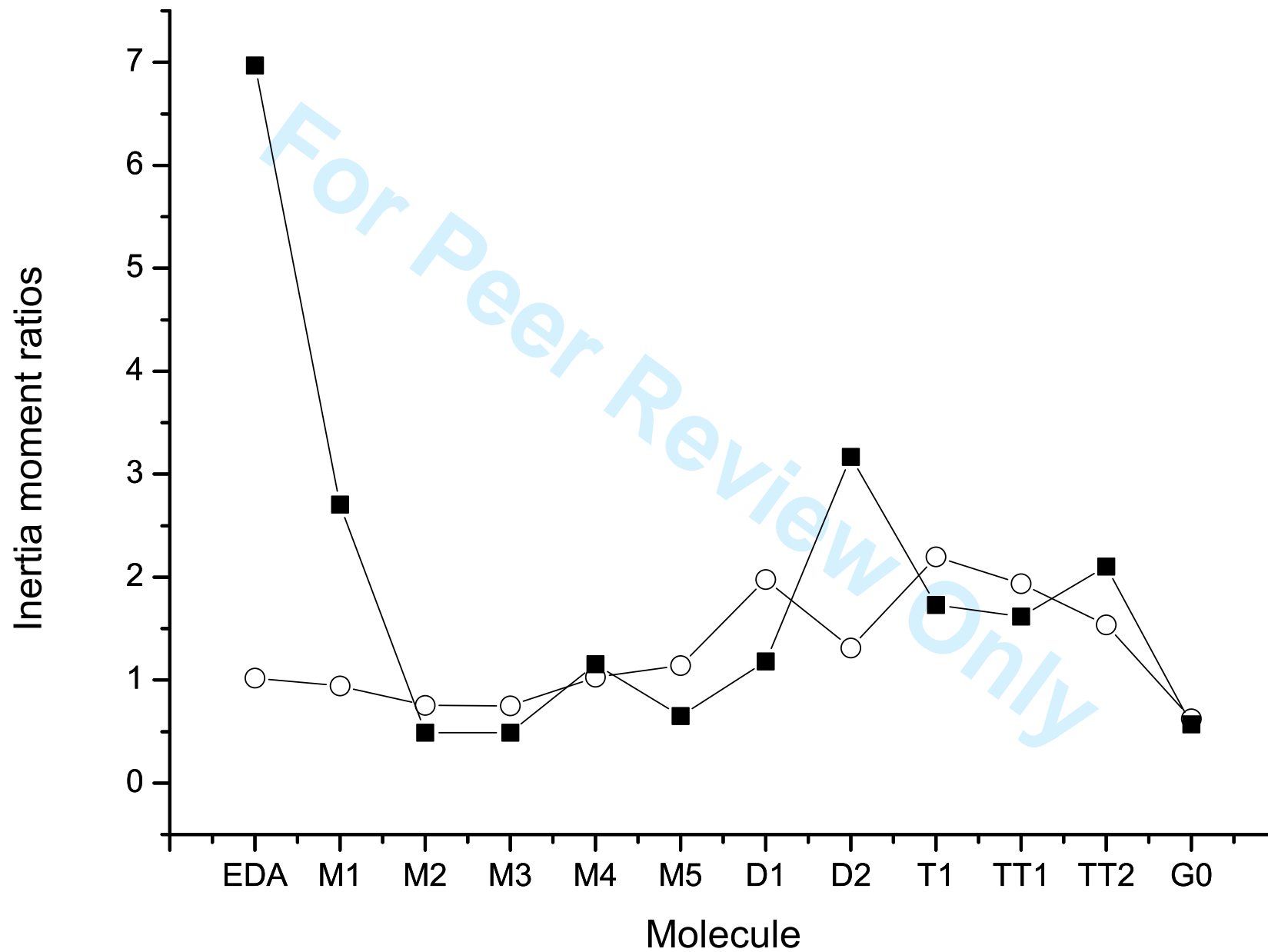
Figure 10. Shannon entropy in Hilbert space, $H(A)$ from Eq. 9 (stars), and the total Energy values at the HF/3-21G* level in a.u. (empty circles) for the G0-precursors and generations G0 through G3. E stands for the EDA molecule.

Figure 11. Kullback-Leibler entropy in Hilbert space, $H(A|B)$ from Eq. 10 (stars), and the total Energy values in a.u. at the HF/3-21G* level (empty circles) for the G0-precursors and generations G0 through G3. E stands for the EDA molecule.

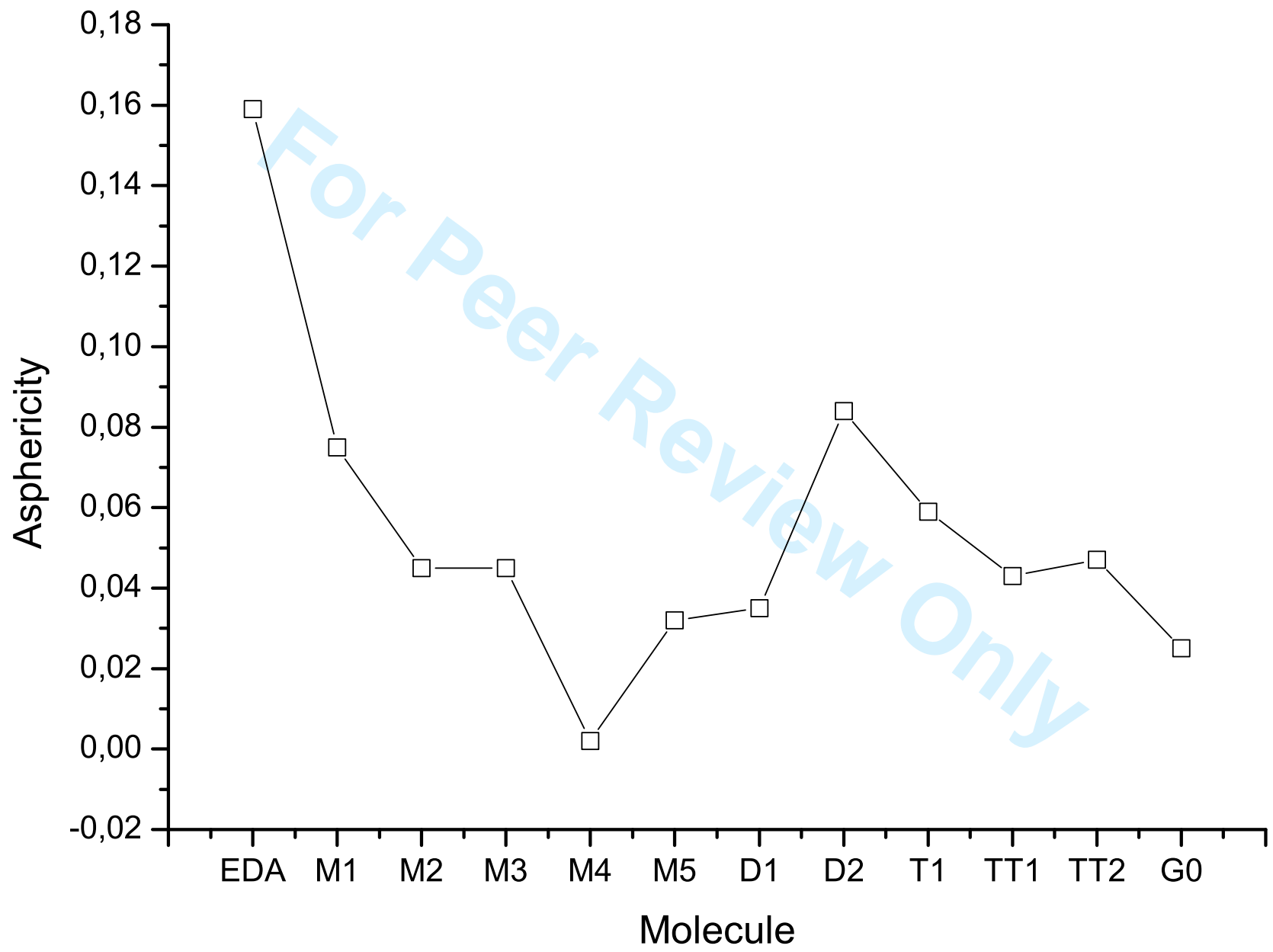


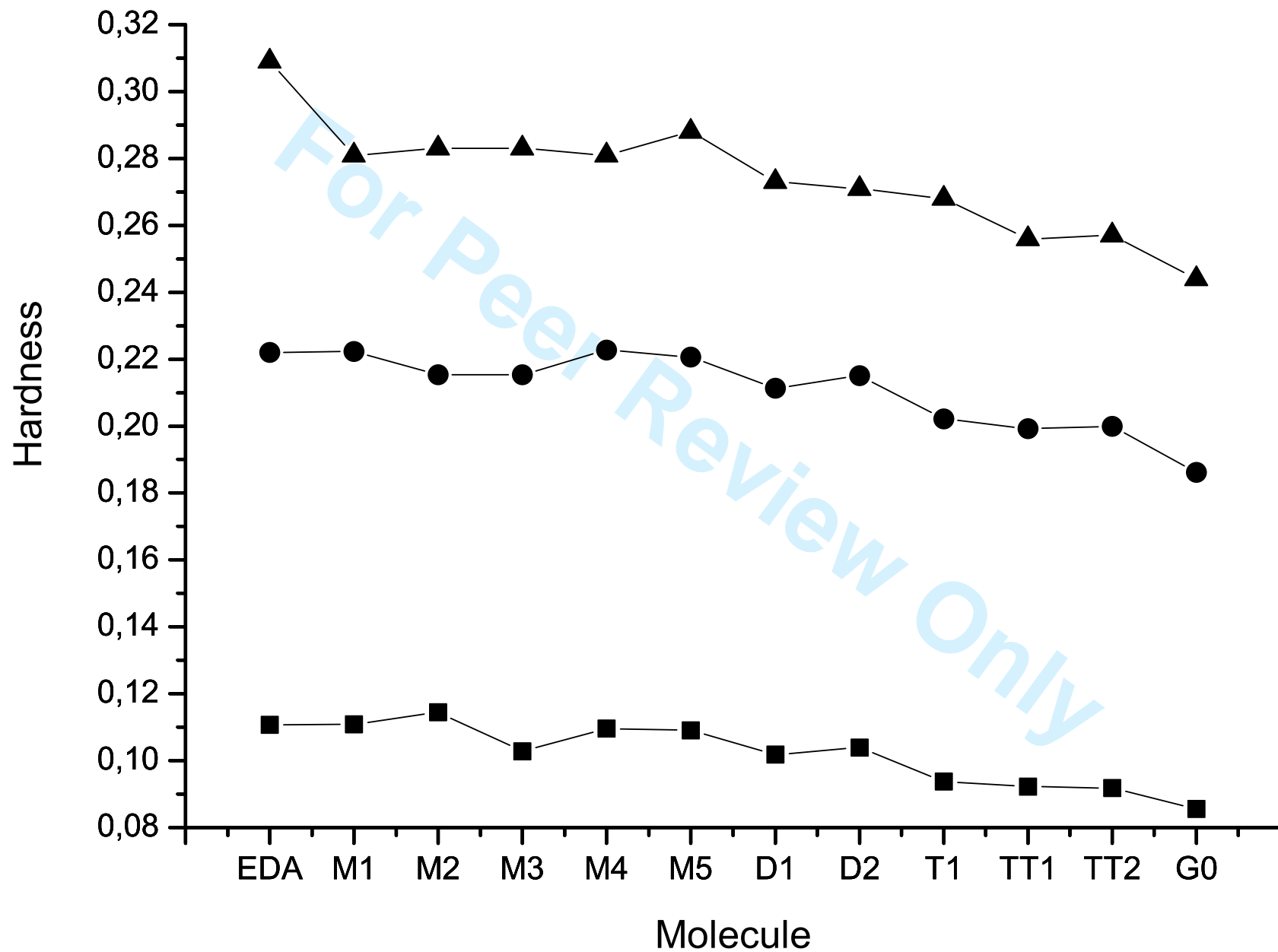
1
2
3
4
5
6
7
8
9
10
11
12
13
14
15
16
17
18
19
20
21
22
23
24
25
26
27
28
29
30
31
32
33
34
35
36
37
38
39
40
41
42
43
44
45
46
47
48
49



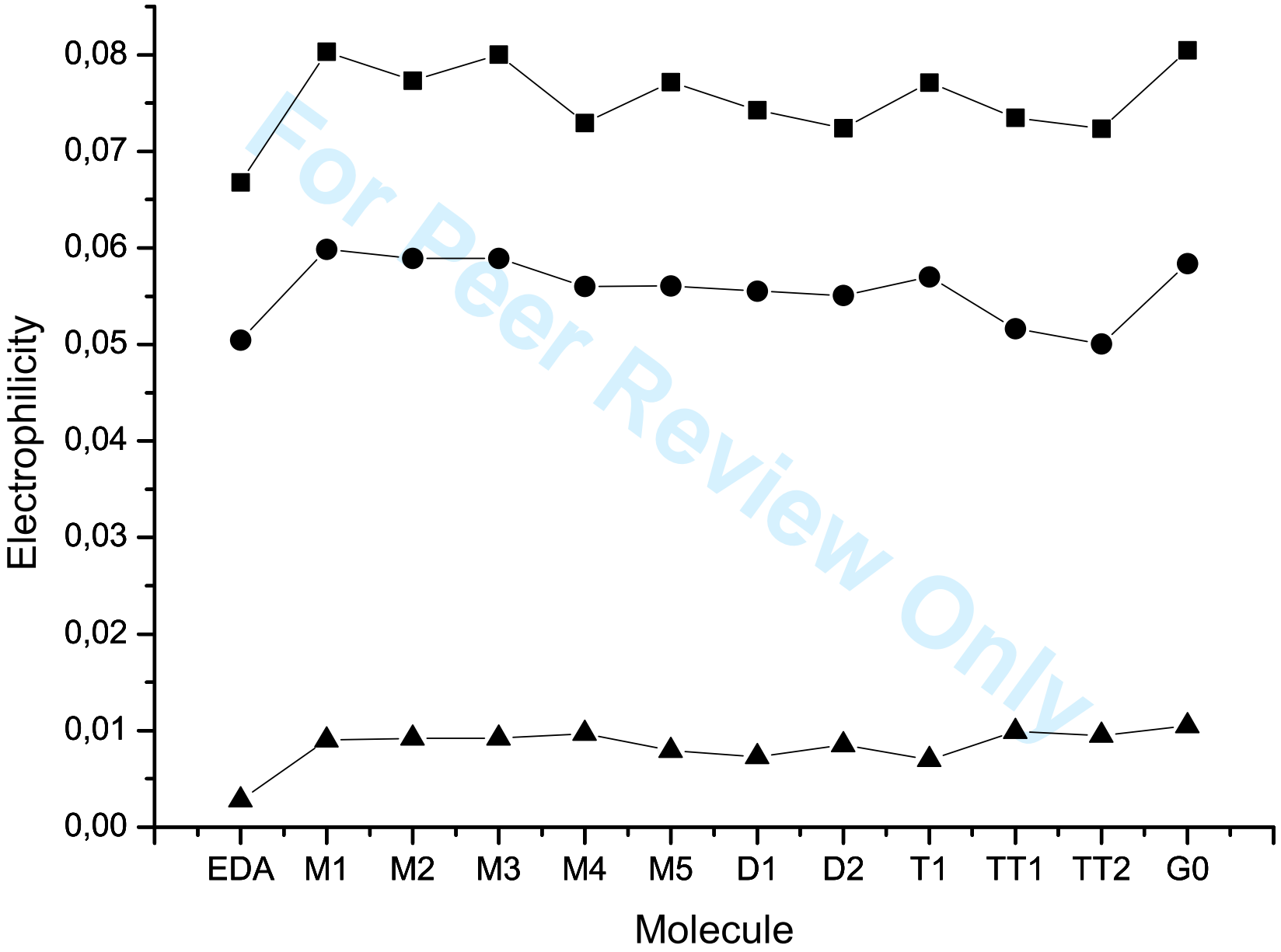


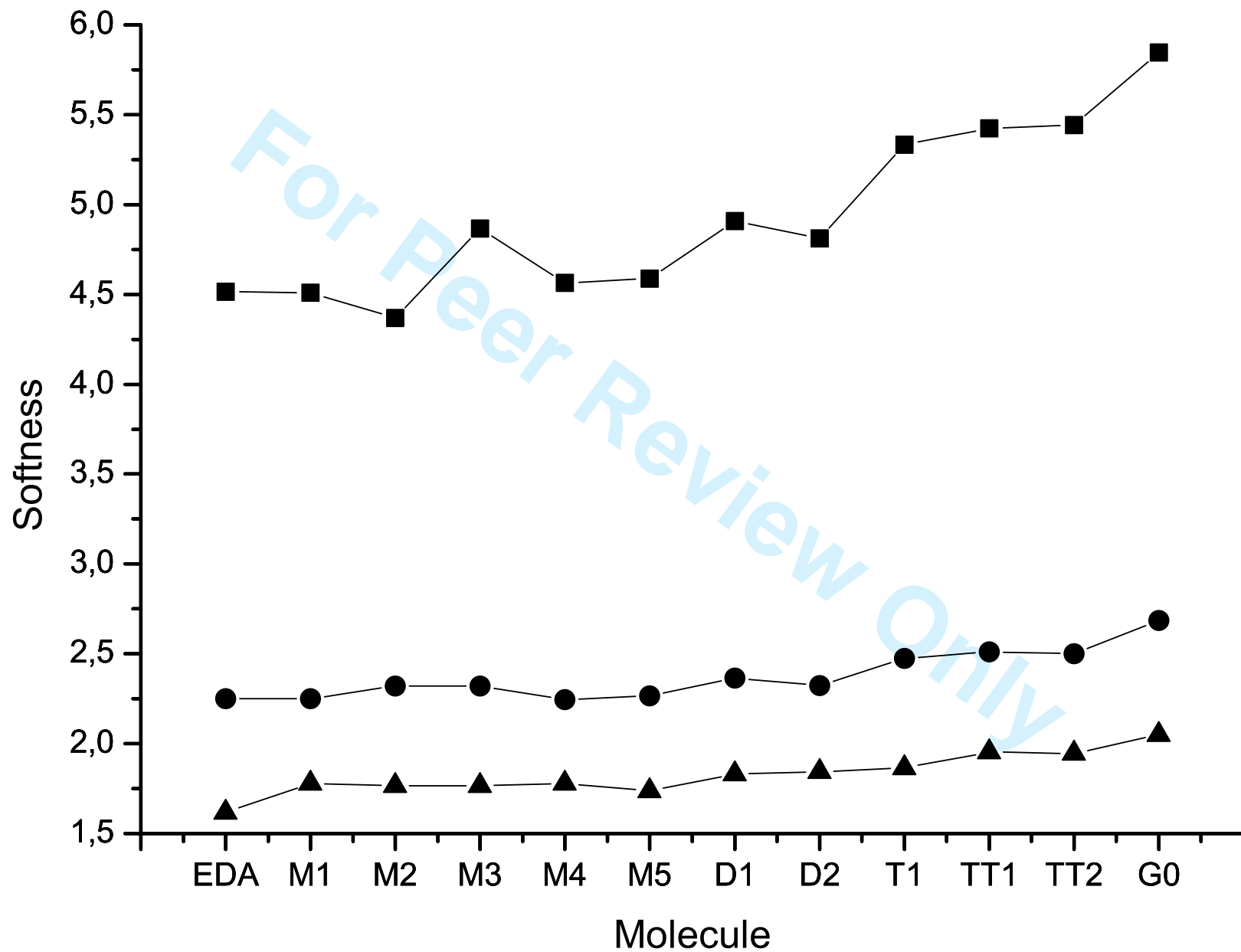
1
2
3
4
5
6
7
8
9
10
11
12
13
14
15
16
17
18
19
20
21
22
23
24
25
26
27
28
29
30
31
32
33
34
35
36
37
38
39
40
41
42
43
44
45
46
47
48
49



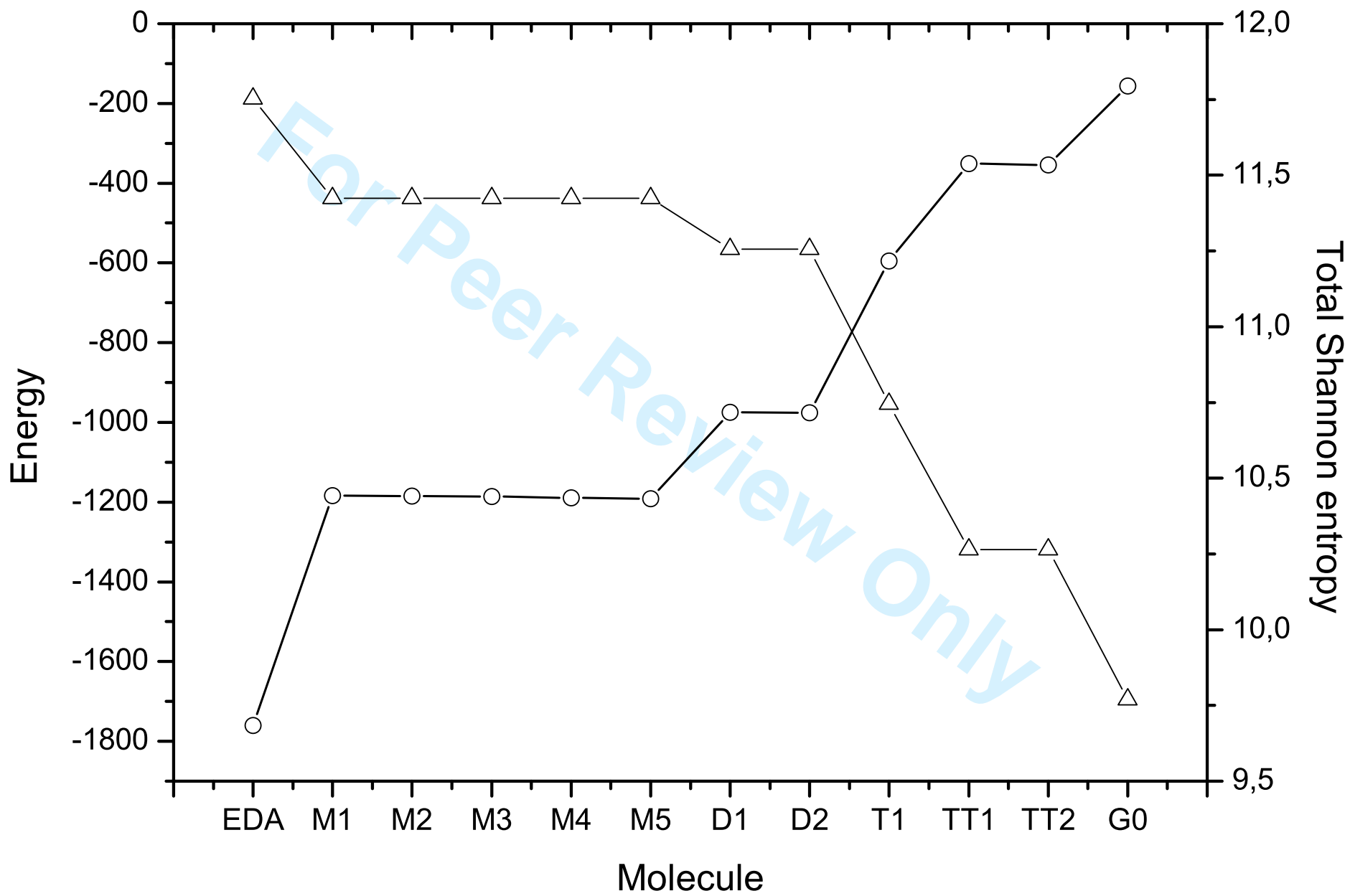


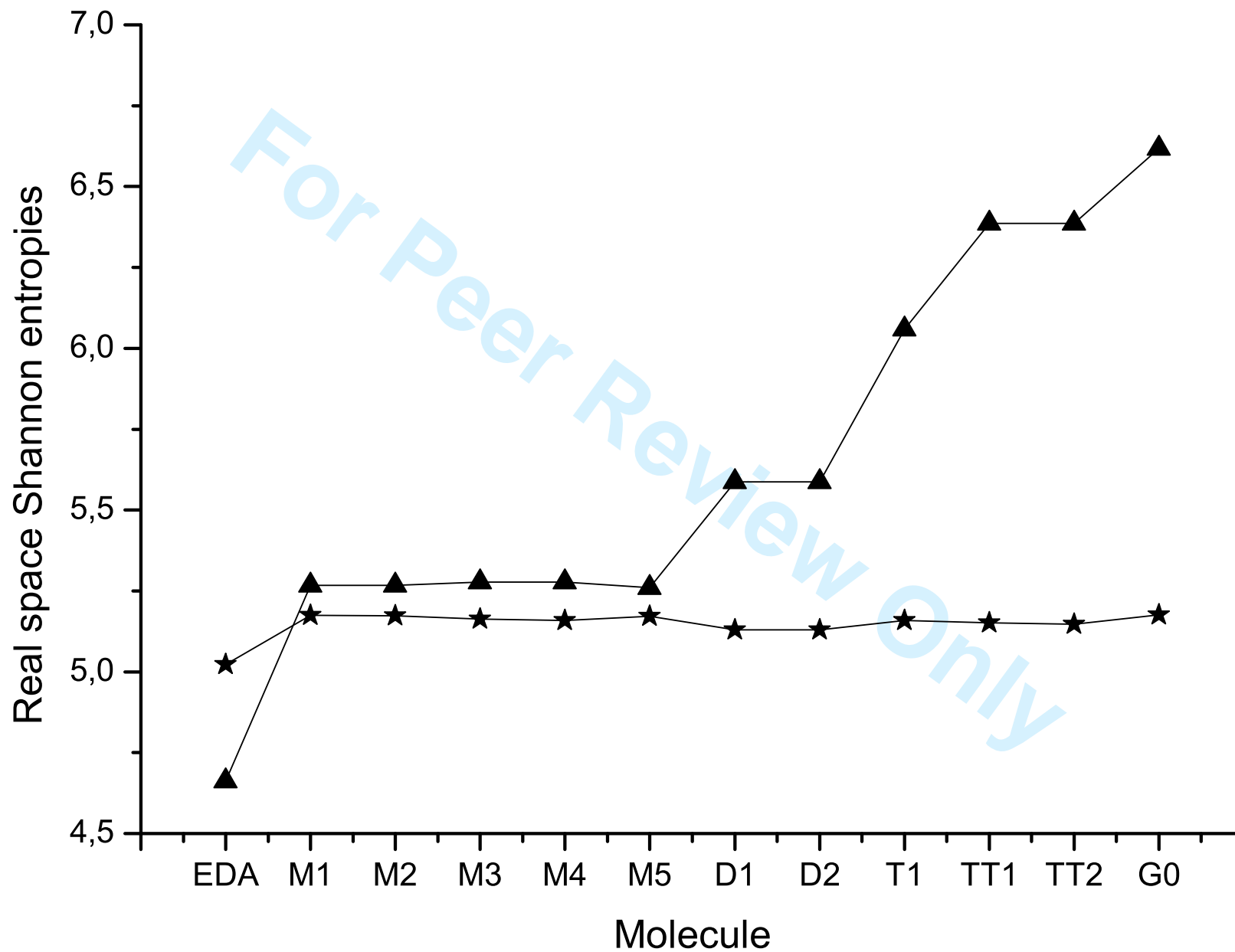
1
2
3
4
5
6
7
8
9
10
11
12
13
14
15
16
17
18
19
20
21
22
23
24
25
26
27
28
29
30
31
32
33
34
35
36
37
38
39
40
41
42
43
44
45
46
47
48
49





1
2
3
4
5
6
7
8
9
10
11
12
13
14
15
16
17
18
19
20
21
22
23
24
25
26
27
28
29
30
31
32
33
34
35
36
37
38
39
40
41
42
43
44
45
46
47
48
49





1
2
3
4
5
6
7
8
9
10
11
12
13
14
15
16
17
18
19
20
21
22
23
24
25
26
27
28
29
30
31
32
33
34
35
36
37
38
39
40
41
42
43
44
45
46
47
48
49

